Title

LEED INTENSITY ANALYSIS OF THE STRUCTURES OF CLEAN Pt(111) AND OF CO ADSORBED ON Pt(111) IN THE c(4x2) ARRANGEMENT

Authors

Ogletree, D.F.
Hove, M.A. Van
Somorjai, G.A.

Publication Date

1985-10-01

Lawrence Berkeley Laboratory
UNIVERSITY OF CALIFORNIA

Materials & Molecular Research Division

Submitted to Surface Science

LEED INTENSITY ANALYSIS OF THE STRUCTURES OF CLEAN Pt(111) AND OF CO ADSORBED ON Pt(111) IN THE c(4x2) ARRANGEMENT

D.F. Ogletree, M.A. Van Hove, and G.A. Somorjai

October 1985

Prepared for the U.S. Department of Energy under Contract DE-AC03-76SF00098

DISCLAIMER

LBL-19920

LEED Intensity Analysis of the Structures of Clean Pt(111) and of CO Adsorbed on Pt(111) in the c(4x2) Arrangement

D. F. Ogletree, M. A. Van Hove, G. A. Somorjai

Materials and Molecular Research Division
Lawrence Berkeley Laboratory
and the Department of Chemistry
University of California
Berkeley, CA 97420

Submitted to Surface Science

October, 1985

This work was supported by the Director, Office of Basic Energy Research, Office of Basic Energy Sciences, Materials Sciences Division of the U.S. Department of Energy under Contract No. DE-AC03-76SF00098."

ABSTRACT:

The surface structures of clean Pt(111) and of CO adsorbed on Pt(111) with c(4x2) periodicity at one-half monolayer coverage are investigated by a dynamical LEED intensity analysis of measured I-V curves. The clean Pt(111) structure is confirmed to be nearly indistinguishable from the truncated bulk structure (within ~0.025Å). The c(4x2) unit cell contains one CO molecule adsorbed on a top site and one CO molecule adsorbed on a bridge site, both molecules being perpendicular to the surface. This is only the second LEED structure determination of multi-site molecular adsorption. The CO molecules have metal-carbon bond lengths of 1.85±0.1Å and 2.08±0.07Å for the top and bridge sites respectively, and the same carbon-oxygen bond length of 1.15±0.05Å. Trends relating bond lengths and vibration frequencies for CO adsorption on various metal surfaces are presented. In particular, the CO stretch frequency decreases as the metal-carbon bond length increases, which in turn increases as the carbon-metal coordination number increases.

1. INTRODUCTION

The adsorption of CO on the Pt(111) surface has been the subject of many studies using a variety of techniques. These include Thermal Desorption Spectroscopy (TDS),[1-3] work-function measurements,[2,4] Angle-Resolved Photoelectron Emission Spectroscopy (ARPES),[5,6] Infrared Reflection-Absorption Spectroscopy (IRAS),[4,7] High-Resolution Electron Energy Loss Spectroscopy (HREELS),[1,3,8-10] and the analysis of Low Energy Electron Diffraction (LEED) patterns.[1,2]

Earlier work has found that the CO molecule remains intact on the Pt(111) surface,[1] and bonds to the surface through the carbon atom, with the molecular axis perpendicular to the surface.[5,6] Vibrational measurements[1,3,8-10] show that CO bonds to one-fold coordinated top sites on Pt(111) at low CO coverages. At higher coverages two-fold coordinated bridge sites are also occupied. At $T \geq 150$ K a temperature-dependent IR absorption peak, assigned to three-fold coordinated hollow sites, is observed in addition to peaks assigned to top and bridge sites.[7] At a CO coverage near 0.5 ML (monolayers in molecules per surface metal atoms) a sharp c(4x2) LEED pattern is seen for $T \leq 300$ K, which is commonly interpreted as consisting of equal numbers of CO molecules adsorbed in top and bridge sites.

There remain a number of questions about the CO-Pt(111) system. A diffuse $(\sqrt{3}x\sqrt{3})R30°$ LEED pattern is observed for T ~150-300 K at CO coverages around 0.33 ML.[1,3] More recent studies show two complex and well-ordered LEED patterns and an intermediate pattern at coverages of 0.17 and 0.33 ML with T~100 K,[1,11] although a third study under similar

conditions did not show these patterns.[7] For coverages above ~0.5 ML a series of complex LEED patterns is observed. This series has been interpreted either in terms of compressed quasi-hexagonal CO layers occupying low-symmetry sites,[2,9] or, more credibly, as combinations of domain walls and anti-phase domains of simple structures.[10,12–14]

The clean Pt(111) surface itself has already been the subject of several structural determinations with LEED[15–21] and with Medium- and High-Energy Ion Scattering (MEIS and HEIS).[21–22] The LEED results are unsatisfactory in that the agreement between calculated and experimental I-V curves is less good than for other clean, unreconstructed metal surfaces (e.g. Al(110)[23] and Cu(110)[24]). This has remained true despite extensive variations of various non-structural and some structural parameters.[20] Here we investigate further variations of structural parameters and examine whether some non-structural parameters can be improved.

We report detailed dynamical LEED analyses of both the clean Pt(111) surface and the c(4x2)-2CO structure at ½-monolayer coverage. The clean Pt(111) structure will be of value in various planned structural determinations involving a series of molecules adsorbed on this substrate, starting with the CO structure examined here. The c(4x2)-2CO adsorption structure itself enables us to establish a firm reference point for the interpretation of the less well understood CO structures at lower and higher coverages, and to provide in addition bond length and bond angle information. At the same time, our result serves to verify the well-known empirical relationship between CO stretch frequency and CO

adsorption site[12–14,25] for the case of the Pt(111)-c(4x2)-2CO structure. This relationship was first established for metal-carbonyl clusters and has already been verified by LEED intensity analyses on several other single-crystal metal surfaces, namely Ni(100),[26–29] Cu(100),[26] Pd(100),[30–31] Rh(111),[32–34] and Ru(0001)[35] for adsorption in top,[26,32–34] bridge,[30–31,33] and hollow sites.[34] This study is only the second structure determination for molecules simultaneously adsorbed in more than one site. The first such study also concerned CO, but adsorbed on Rh(111) in a (2x2) lattice.[33] A further such study, recently completed, concerns the coadsorption of CO and benzene on Rh(111).[34]

2. EXPERIMENT

Our experiments were performed in an ion-pumped, stainless steel UHV system, equipped with a quadrupole mass spectrometer, an ion bombardment gun, and a four-grid Varian LEED optics. An off-axis electron gun and the LEED optics were used for Auger measurements. We used a platinum (111) crystal 6 mm x 7 mm x 0.7 mm in size, spot-welded to strips of tantalum foil. The crystal could be cooled to ~140 K by conduction from a pair of liquid nitrogen cold fingers or heated resistively to ~1500 K. Temperatures were measured by a 0.005" chromel-alumel thermocouple spot-welded to one edge of the platinum crystal. The system base pressure was ~1×10^{-9} torr. CO was the main component of the background residual gas.

The platinum crystal was cleaned by a combination of 500 eV argon ion bombardment and annealing at 1000 K. Residual carbon was removed by reaction with 2×10^{-7} torr oxygen at 1000 K, followed by flashing the crystal above 1300 K in vacuum. The principal impurities were sulfur and carbon, with trace amounts of calcium, silicon, and phosphorus. The above cleaning procedure was sufficient to reduce the surface concentration of impurities below the Auger detection threshold. Careful examination of the clean platinum LEED pattern with particular attention to the diffuse background intensity provided an additional check of the sample cleanliness.

The LEED optics and vacuum chamber were enclosed by two sets of Helmholtz coils to minimize magnetic fields near the crystal. These coils were adjusted until there was no significant deflection of the specularly reflected beam over the 20 to 200 eV energy range used for LEED I-V measurements. There were no exposed insulators or ungrounded conductors in the vicinity of the crystal, in order to minimize electrostatic fields. The LEED electron gun was operated in the space-charge limited mode, so that the beam current increased monotonically and approximately linearly over the voltage range used. At 200 eV the beam current was ~3.5 μ-amps. The intensity-energy curves were normalized with respect to incident beam current.

The crystal was mounted on a manipulator capable of independent azimuthal and co-latitude rotations. The crystal surface was oriented with the (111) face perpendicular to the azimuthal rotation axis as determined by visual comparison of the intensities of symmetry related

substrate beams. It is possible to see deviations from normal incidence of less than 0.2° with this method. The accuracy of the orientation was confirmed by the close agreement of I-V curves for symmetry-related beams. The off-normal incidence angles were set by rotating the crystal away from the experimentally determined normal-incidence position using a scale inscribed on the manipulator.

LEED data were collected using a high-sensitivity vidicon TV camera with a f/.85 lens. The data were recorded on video tape for later analysis. The entire diffraction pattern was analyzed using a real-time video digitizer interfaced to an LSI-11 microcomputer. Sixteen consecutive video frames at constant energy were summed to improve the signal/noise ratio, then an image recorded at zero beam voltage was subtracted to correct for the camera dark current and stray light from the LEED screen or filament. I-V curves were generated by a data reduction program that locates diffraction spots in the digitized image, integrates the spots, and makes local background corrections.[15]

CO Adsorption

A c(4x2) LEED pattern, illustrated in Figure 1, was formed by flashing the clean Pt(111) crystal to 550 K and then dosing the surface with CO as it cooled to 150 K. The crystal was exposed to a nominal 5×10^{-8} torr of CO for 20 seconds, starting as the crystal cooled through ~270 K. The crystal was located 10 cm away from a stainless steel doser tube 0.15 cm in diameter. With this arrangement a 0.1 Langmuir exposure based on the uncorrected ion gauge reading corresponds to a 1 Langmuir

exposure in the work of Ertl et al.[2] This procedure gave a reproducible, well ordered c(4x2) structure.

The electron beam easily damages the c(4x2) structure. During I-V data collection the electron beam exposure was limited to 45 μamp-seconds. This limit was determined to cause no significant beam-induced changes in the c(4x2) diffraction pattern or intensities. A full set of I-V curves was recorded in ~100 seconds using the video LEED system. A running total of the electron beam exposure was kept, and data acquisition stopped when the exposure limit was reached. The crystal was then flashed over 550 K, desorbing the CO, and a new CO exposure was made before data acquisition was resumed. All of the I-V data were collected at a crystal temperature of ~150 K to optimize the contrast in the LEED pattern. After each set of I-V data was collected the crystal was checked by Auger spectroscopy for contamination, with particular attention given to carbon on the surface.

I-V Curves

The I-V data for the c(4x2)-2CO structure on Pt(111) were collected at normal incidence and with the incident electron beam rotated 5° and 15° from normal incidence, such that the surface projection of the k-vector points toward the (1,0) beam, maintaining one mirror plane of symmetry. Two independent experiments were performed at each angle, and the final I-V curves are an average of symmetrically equivalent beams

from both data sets. The energy range used was 20-200 eV. The normal-incidence data set has I-V curves for 9 independent beams with 30 significant peaks over a cumulative 1000 eV energy range. The 5° and 15° data sets each have 14 independent beams with more than 35 peaks over a cumulative energy range greater than 1300 eV at each angle.

3. THEORY

We have chosen established multiple-scattering methods to calculate LEED intensities.[37] Namely, the Combined-Space Method was applied, with Reverse Scattering Perturbation within the CO overlayer (which contains two inequivalent molecules in each unit cell). Renormalized Forward Scattering was used to stack the metal layers and the overlayer. This approach was also used in a comparable study of CO adsorbed simultaneously in near-top and bridge sites on Rh(111).[33] No further approximations in the multiple-scattering treatment were made in this study.

The phase shifts describing the electron scattering by platinum atoms were obtained in part from a new relativistic atomic potential.[38] This potential was chosen because it gave a slightly better agreement with LEED experiment for clean Pt(111) than a previously used potential due to Andersen.[20] Calculations for CO on Pt(111) were performed only with this new potential. The CO scattering phase shifts are the same as used previously in studies of CO adsorbed on other metal surfaces.[30-34] The spherical-wave expansion was cut off at $\ell_{max}=7$ for the clean-surface case and at $\ell_{max}=5$ for the overlayer case. The imaginary part of the

muffin-tin potential was set proportional to $E^{1/3}$, with a value of 3.8 eV at a kinetic energy of 90 eV. The Debye temperature was initially chosen as 302 K for the clean Pt(111) surface, the optimum value found in reference 12, and 255 K in all Pt layers in the CO-covered surface, closer to the bulk Debye temperature of about 234 K. The C and O atoms were initially given the mean square vibration amplitudes of the underlying Pt atoms, multiplied by 2 to take a possible surface enhancement into account.

For the comparison between experiment and theory, a set of five R-factor formulas and their average was used, as described previously and used by us in many prior LEED analyses.[30-34]

4. CLEAN Pt(111)

As indicated in Section 1, previous LEED intensity studies of Pt(111) were not fully satisfactory. In reference 20, various non-structural parameters of the LEED theory were systematically varied, as well as the topmost interlayer spacing. Also, a potential with relativistic corrections was tried, but yielded no improvement.[12] Here we consider the variation of other structural parameters and of additional thermal vibration amplitudes. A new platinum scattering potential is used, which includes relativistic effects (subsequently spin-averaged) and was generated by Wang.[38] This potential yields slightly better results than a previous potential by Andersen.[15-16,20]

The ion scattering data indicate that the Pt(111) structure deviates from the bulk geometry by a possible small expansion of the top interlayer spacing of 0.03±0.01 Å[21] or 0.03±0.02 Å.[22] No deviation from the bulk position is found in the direction parallel to the surface, with a similar accuracy of about 0.01-0.02 Å. We have investigated multilayer relaxations of the three topmost interlayer spacings d_{12}, d_{23} and d_{34}. We have allowed d_{12} and d_{23} to vary by up to ±0.1 Å from the bulk value (2.2655 Å), while d_{34} was given either the bulk value or a contraction by 0.05 Å.

Assuming identical vibration amplitudes in all atomic layers (Θ_D= 302 K) and using the Wang potential, the optimal changes Δd_{12}, Δd_{23} and Δd_{34} in these spacings are: Δd_{12}=0.0±0.025 Å, Δd_{23}=-0.025±0.025 Å and Δd_{34}=0.0±0.05 Å, where a negative sign implies contraction. The optimum muffin-tin zero level was V_o=14±0.5 eV below vacuum. This structure yields a five-R-factor average of R=0.24; the corresponding Zanazzi-Jona and Pendry R-factor values are 0.29 and 0.50. A layer dependence of the vibration amplitudes had a negligible effect on the R-factors.

We also investigated relaxations parallel to the surface, since the clean Ir, Pt and Au surfaces tend to reconstruct,[39] including Au(111) but not Pt(111). The Pt(100) and Au(100) reconstruction involves, in the topmost layer only, average bond lengths reductions parallel to the surface by about 2%. Thus, for Pt(111), we allowed a 2% contraction parallel to the surface, but in <u>all</u> layers, since no superlattice

structure is seen which would indicate a layer-dependent contraction (such a contraction deep into the surface would most likely have been detected in MEIS or HEIS[13-14]). This however increased the R-factor from 0.240 to 0.251. Finally, we allowed the topmost layer to shift rigidly parallel to the surface by 0.2 Å (with three 120°-rotated domains). The R-factor then rose even more.

As a result, for Pt(111) we detect no parallel relaxation, and no unambiguous perpendicular relaxation from the bulk structure within ~0.025 Å.

We may rule out any non-bulk lattice terminations, such as hcp-stacking, on the basis of MEIS and HEIS results, which would have unambiguously detected such gross atomic displacements.[13-14]

5. TEST STRUCTURES FOR CO ADSORPTION

We have examined a variety of adsorption structures for CO in the c(4x2) unit cell. They all assume a coverage of Θ=½ ML and they involve the following combinations of CO adsorption sites:

a) ¼ ML in top sites and ¼ ML in bridge sites (as illustrated in Fig. 2);

b) ¼ ML in top sites and ¼ ML in fcc-type hollow sites;

c) ¼ ML in top sites and ¼ ML in hcp-type hollow sites;

d) ¼ ML in bridge sites and ¼ ML in fcc-type hollow sites;

e) ¼ ML in bridge sites and ¼ ML in hcp-type hollow sites;

f) ¼ ML in top sites; the remaining ¼ ML is left out of the calculation to simulate a highly disordered state of these CO molecules. This is a rough test of the hypothesis[7] that for T≳150 K bridge-site CO molecules switch easily and randomly to both nearby hollow sites, as illustrated at bottom right in Fig. 2.

In all the above-mentioned cases the substrate structure was kept bulk-like, since no significant relaxations are apparent in the clean surface. The CO molecular axes were kept perpendicular to the surface plane, as suggested by ARPES measurements.[5-6] In the structures (a)-(e), various combinations of different heights of the inequivalent CO molecules above the Pt(111) surface were examined. The C-O bond length was assumed identical for molecules in both sites in each trial structure: it was fixed at 1.15 Å for the structures (b)-(f) but varied independently of other parameters for the structures (a), with the values 1.10, 1.15 and 1.20 Å. In total, 146 different geometries were investigated. All of these were analyzed with the normal-incidence LEED data, while 20 structures of type (a) were also evaluated with the off-normal incidence data.

6. STRUCTURAL RESULTS FOR CO ADSORPTION

The LEED comparisons strongly favor the top-bridge combination of adsorption sites for Pt(111)-c(4x2)-2CO, i.e. structure (a). The optimal structural parameters are: C-O bond length of 1.15±0.05 Å for both adsorption sites; and metal-carbon interlayer spacings of 1.85±0.10 Å and 1.55 ±0.10Å for top- and bridge-site molecules, respectively, which corresponds to metal-carbon bond lengths of 1.85±0.10 Å and 2.08±0.07 Å, respectively. The optimal muffin-tin zero level, assumed layer-independent, is found to be 12±1 eV. The minimized value of the five-R-factor average is 0.29, while the corresponding Zanazzi-Jona and Pendry R-factor values are 0.50 and 0.61. (These values are obtained by averaging the results for two of the three angles of incidence, θ=0° and θ=5°. The R-factor results for θ=15° were not included, because of erratic values in the Zanazzi-Jona R-factor close to the presumed minimum. The other R-factors at 15°, however, confirmed the structure found with the 0° and 5° data.)

R-factor contour plots for θ=0° and θ=5° are presented in Fig. 3. For comparison, the corresponding R-factor values for Rh(111)-(2x2)-3CO, which also contains CO molecules in two different sites in the unit cell, are 0.19, 0.25, and 0.47 for the five-R-factor average, the Zanazzi-Jona R-factor and the Pendry R-factor, respectively. These values are rather better than for the case of the Pt(111) substrate, mainly because the clean Rh(111) surface gives much better agreement between LEED theory and experiment than does the clean Pt(111) surface.

7. DISCUSSION

Clean Pt(111) Surface

We have attempted to improve the agreement between theory and experiment for Pt(111) by allowing additional structural and non-structural changes. Only a new scattering potential yielded an improvement, which was slight: R-factor reduction from 0.247 to 0.240 from the Andersen potential[10,12] to the Wang potential.[24] There remain discrepancies and their origin may lie outside of the surface model used at present in LEED theory, e.g. non-uniform damping, unusual vibration properties or small non-periodic distortions.

Our structural result for Pt(111) confirms earlier LEED results,[15-26] namely a bulk structure within the uncertainty of the method, i.e. within ~0.025 Å. Our new result also closely matches values obtained with Ion Scattering.[22-23]

Pt(111)-c(4x2)-2CO

The binding sites which we obtain for a half monolayer of CO adsorbed on Pt(111), namely top and bridge, confirm the expectations based on vibrational studies for T<150 K.[1,3,8-10] This follows from the correlation between C-O stretch vibration frequency and adsorption site which was mentioned in Section 1.[12-14,25] This relationship is exhibited in Fig. 4, where the observed frequencies are shown for each CO structure for which a detailed structural determination has been carried out by

LEED: the LEED result in each case has confirmed the vibrational assignment. The present work thus also verifies the validity of this correlation on Pt(111).

Our structure determination supports the ARPES result that CO adsorbs perpendicularly to the metal surface in this system. Namely, a tilted CO would yield the observed C-O interlayer spacing of 1.15Å only with an abnormally elongated C-O bond length.

As was also mentioned in Section 1, there is evidence from vibrational measurements[4] that a fair fraction of the bridge-sited CO molecules shifts to different, possibly hollow sites as the temperature is raised above 150 K. The poor fit of our calculation with only a ¼ ML of top-site CO molecules supports the contention that the majority of CO moleculesis located at top and bridge sites at T=150 K.

We may compare the metal-carbon and carbon-oxygen bond lengths obtained in this study with corresponding values for other substrates and for metal-carbonyl clusters,[40] cf. Fig. 5. Since different metals with different atomic radii are involved, we also compare effective carbon radii obtained by subtracting from the metal-carbon bond length half the metal-metal distance of the bulk metal or of the cluster, as appropriate, cf. Fig. 6. Included in the comparison of Figs. 5 and 6 is the first CO adsorption result by LEED involving a threefold hollow site on a surface.[34] This is obtained on Rh(111) when CO is coadsorbed with benzene. The effect is presumably similar to that of CO and potassium coadsorption, which also appears to favor hollow site adsorption of CO on

several metal surfaces. Fig. 5 and especially Fig. 6 exhibit a good correlation between structural results for CO adsorption. First, good agreement is seen between results at surfaces and results in clusters. Second, the structures can be grouped for the three types of adsorption sites, exhibiting clearly the trend toward a larger metal-carbon bond length as the metal coordination number increases from 1 to 2 to 3.

In Fig. 7 we correlate the metal-carbon and carbon-oxygen bond lengths determined at surfaces with the CO stretching frequencies as measured by HREELS or IRAS (correlations with the metal-carbon stretch frequency are much less apparent). Fig. 7a clearly illustrates two trends: the C-O stretch frequency reduction and metal-carbon bond-length expansion as the metal coordination increases from 1 to 2 to 3. Within a group of results for the same site (e.g. top site) the scatter of the results is too large to discern a trend. One would expect an increase in CO stretch frequency with increasing metal-carbon bond length, reflecting a strengthening CO bond. But additional factors such as substrate, work function and coverage dependence can cause large variations. In Fig. 7b the same trends are discernible, although here the uncertainty in the bond length determination (0.05 to 0.1 Å) is comparable to the effect we are seeking. For comparison, Fig. 7b indicates a clear trend for small CO-containing molecules, in which the C-O bond length is known with higher accuracy (~0.01 Å).

We may fit the data of Fig. 7 to obtain an empirical linear relationship between bond length and frequency. The straight lines shown in Fig. 7 can be approximated by the equations:

$$d_{MC}[\text{Å}] = -6.25 \times 10^{-4} \times \nu_{CO}[cm^{-1}] + 3.18,$$
$$d_{CO}[\text{Å}] = -2 \times 10^{-4} \times \nu_{CO}[cm^{-1}] + 1.56.$$

(Note that for d_{CO} we have fit the non-surface data points of Fig. 7b.) It is clear that the M-C bond length shows a much stronger correlation with C-O stretch frequency than does the C-O bond length. These relationsips may be used to obtain an approximate prediction of M-C and C-O bond lengths, given the C-O stretch frequency.

8. CONCLUSIONS

The structure of clean Pt(111) is confirmed to be virtually indistinguishable from a simple truncation of the bulk structure, within ~0.25 Å. The agreement between theory and experiment is, however, less satisfactory than for many other metal surfaces.

The structure of CO adsorbed at a coverage of ½ monolayer on Pt(111) is confirmed to consist of simultaneous top and bridge site occupation (with CO axes perpendicular to the surface), in agreement with HREELS and IRAS data. The bond lengths compare very well with those known in metal-carbonyl clusters and for CO adsorption on other single-crystal metal surfaces. Such comparisons show clear correlations between C-O stretch frequency reduction and binding site, and between metal-carbon bond length and binding site.

ACKNOWLEDGEMENTS

This work was supported by the Director, Office of Energy Research, Office of Basic Energy Sciences, Materials Science Division, of the U.S. Department of Energy under Contract Number DE-AC03-76SF00098. We also acknowledge supercomputer time provided by the Office of Energy Research of the U.S. Department of Energy.

REFERENCES

1. H. Steininger, S. Lehwald, and H. Ibach, Surf. Sci. 123 (1982) 645.

2. G. Ertl, M. Neumann, and K.M. Streit, Surf. Sci. 64 (1977) 393.

3. H. Hopster and H. Ibach, Surf. Sci. 77 (1978) 109.

4. K. Horn and J. Pritchard, J. Physique 38-C4 (1977) 164.

5. P. Hoffman, S.R. Bare, N.V. Richardson, and D.A. King, Solid State Comm. 42 (1982) 645.

6. M. Trenary, S.L. Tang, R.J. Simonson, F.R. McFeely, Surf. Sci. 124 (1983) 555.

7. B.E. Hayden and A.M. Bradshaw, Surf. Sci. 125 (1983) 787.

8. H. Froitzheim, H. Hopster, H. Ibach and S. Lehwald, Appl. Phys. 13 (1977) 147.

9. A.M. Baró and H. Ibach, J. Chem. Phys. 71 (1979) 4812.

10. N.R. Avery, J. Chem. Phys. 74 (1981) 4202.

11. B. Poelsema, R.L. Palmer, G. Comsa, Surf. Sci. 123 (1982) 152; Surf. Sci. 136 (1983) 1.

12. J.P. Bibérian and M.A. Van Hove, in "Vibrations at Surfaces", Eds. R. Caudano, J.-M. Gilles, and A.A. Lucas, Plenum (New York) 1982, p. 91.

13. J.P. Bibérian and M.A. Van Hove, Surf. Sci. 118 (1982) 443; Surf. Sci. 122 (1982) 600.

14. J.P. Bibérian and M.A. Van Hove, Surf. Sci. 138 (1984) 361.

15. L.L. Kesmodel and G.A. Somorjai, Phys. Rev. B11 (1975) 630.

16. L.L. Kesmodel, P.C. Stair, and G.A. Somorjai, Surf. Sci. 64 (1977) 64.

17. R. Feder, Surf. Sci. 68 (1977) 229.

18. P. Bauer, R. Feder, and N. Müller, Surf. Sci. 99 (1980) L395.

19. R. Feder, H. Pleyer, P. Bauer, and N. Müller, Surf. Sci. 109 (1981) 419.

20. D.L. Adams, H.B. Nielsen, and M.A. Van Hove, Phys. Rev. B20 (1979) 4789.

21. J.A. Davies, D.P. Jackson, N. Matsunami, P.R. Norton, and J.U. Andersen, Surf. Sci. 78 (1978) 274.

22. J.F. Van der Veen, R.G. Smeenk, R.M. Tromp, and F.W. Saris, Surf. Sci. 79 (1979) 219.

23. J.R. Noonan and H.L. Davis, Phys. Rev. B29 (1984) 4349.

24. D.L. Adams, H.B. Nielsen, and J.N. Andersen, Surf. Sci. 128 (1983) 294.

25. R.P. Eischens and W.A. Pliskin, Advan. Catalysis 10 (1958) 1.

26. S. Andersson and J.B. Pendry, Phys. Rev. Lett. 43 (1979) 363; J. Phys. C13 (1980) 3547.

27. M.A. Passler, A. Ignatiev, F. Jona, D.W. Jepsen, and P.M. Marcus, Phys. Rev. Lett. 43 (1979) 360.

28. K. Heinz, E. Lang, and K. Müller, Surf. Sci. 87 (1979) 595.

29. S.Y. Tong, A. Maldonado, C.H. Li, and M.A. Van Hove, Surf. Sci. 94 (1980) 73.

30. R.J. Behm, K. Christmann, G. Ertl, M.A. Van Hove, P.A. Thiel, and W.H. Weinberg, Surf. Sci. 88 (1979) L59.

31. R.J. Behm, K. Christmann, G. Ertl, M.A. Van Hove, J. Chem. Phys. 73 (1980) 2984.

32. R.J. Koestner, M.A. Van Hove, and G.A. Somorjai, Surf. Sci. 107 (1981) 439.

33. M.A. Van Hove, R.J. Koestner, J.C. Frost, and G.A. Somorjai, Surf. Sci. 129 (1983) 482.

34. M.A. Van Hove, R.F. Lin, and G.A. Somorjai, to be published.

35. G. Michalk, W. Moritz, H.Pfnür, and D. Menzel, Surf. Sci. 129 (1983) 92.

36. D.F. Ogletree, J.E. Katz, G.A. Somorjai, in preparation.

37. M.A. Van Hove and S.Y. Tong, "Surface Crystallography by LEED" Springer (Heidelberg) 1979.

38. S.W. Wang, private communication.

39. M.A. Van Hove, R.J. Koestner, P.C. Stair, J.P. Biberian, L.L. Kesmodel, I. Bartoš, and G.A. Somorjai, Surf. Sci. 103 (1981) 189, 218.

40. P. Chini, V. Longoni, and V.G. Albano, Advan. Organomet. Chem. 14 (1976) 285.

Figure Captions

1) LEED patterns of the c(4x2) unit cell formed when 1/2 monolayer of CO is absorbed on a Pt(111) surface. CO was absorbed and the ordered structure formed at 270 K, and then the crystal was cooled to 150 K. Three rotated domains of this unit cell are superimposed in the observed LEED pattern. A schematic diagram of the LEED pattern is shown in (c). Cormally the three domains have approximately equal intensity, (a) and (b). Occasionaly, as in (d), one domain is predominant.

2) The optimum surface for CO in the c(4x2) arrangement on the Pt(111) surface, as determined by dynamical LEED calculation and r-factor analysis. The broken circles in the lower right corner of the figure indicate the CO inter-molecular spacing if a bridge site CO molecule were to move to either 3-fold hollow site.

3) Contour plots of the five-R-factor average as a function of two of the structural parameters in the model of Figure 2. The parameters used are the perpendicular distance between the top-layer metal atoms and the bridge-site carbon atoms, and the perpendicular distance between the top-site and bridge-site carbon atoms. The C-O bond lengths were held at 1.15Å for these plots.

4) The correlation between the C-O stretch frequency (shown as dots), as observed by HREELS or IRAS, and the adsorption site, as determined by LEED structure calculations, for CO adsorbed on metal surfaces.

5) Comparison of metal-carbon and carbon-oxygen bond lengths for CO absorbed on metal surfaces and for CO in metal-carbonyl clusters. Bond lengths for surfaced are as determined by LEED, and the corresponding symbols are labeled with the substrate name. Metal-carbonyl bond lengths are shown with unlabeled symbols. Circles, squares, and triangles indicate top, bridge, and hollow sites, i.e. 1-, 2-, and 3-fold coordinated sites, respectively. The inset legend identifies the metal substrates. The labels 1/3 and 3/4 indicate different coverages of CO in units of monolayers. The label C_6H_6 refers to coadsorption with benzene. Results for top sites, bridge sites and hollow sites are surrounded by enclosing lines for easier identification.

6) As Figure 5, except the metal-carbon bond length is replaced by an effective carbon radius, obtained by subtracting the radius of metal atoms in the cluster or bulk metal substrate.

7) Metal-carbon (a) and carbon-oxygen (b) bond lengths vs. measured C-O stretch frequency, for CO absorbed on surfaces and for a few CO-containing molecules. Labels are as in Figure 5.

Pt (111) – c (4 × 2) – 2CO
LEED Patterns T = 150 K

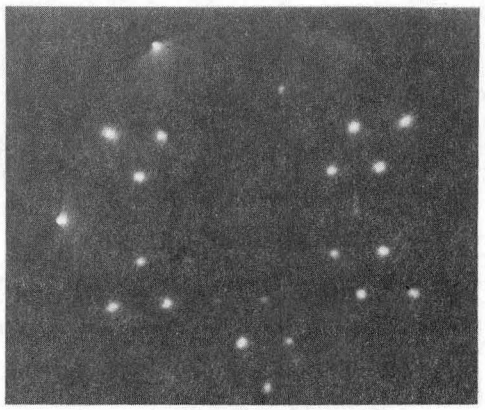

a) 38 eV

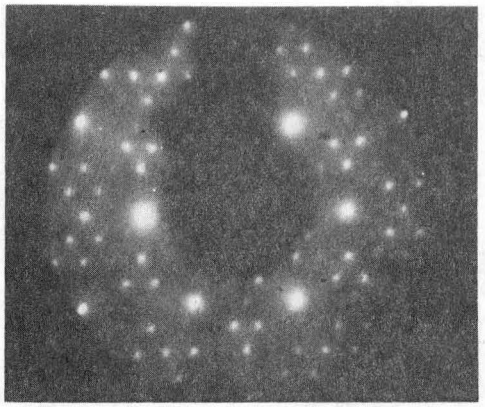

b) 130 eV

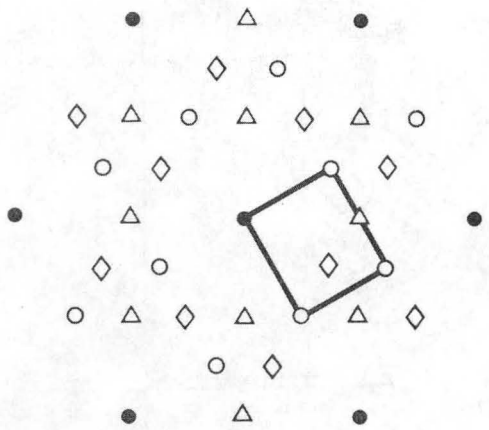

c) LEED Pattern
Schematic

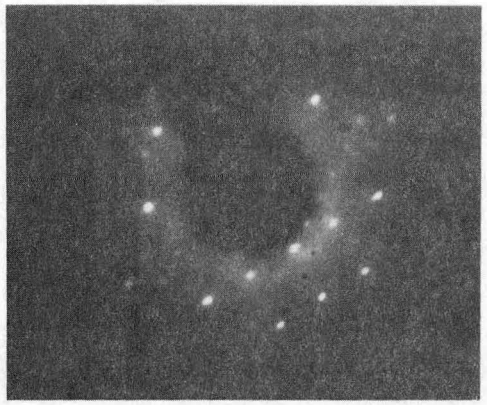

d) 110 eV
One domain
predominant

- ● substrate spots
- ○ 1st domain
- △ 2nd domain
- ◇ 3rd domain

XBB 829-8617A

Fig.1

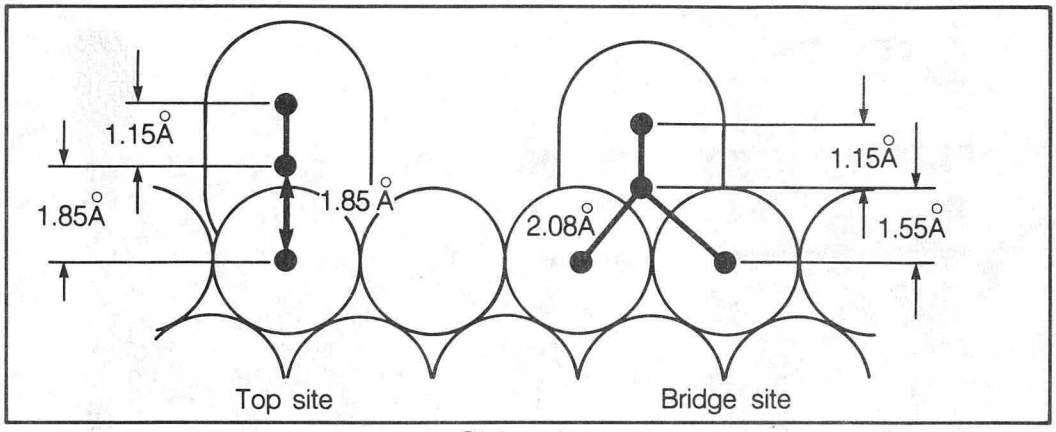

Side view

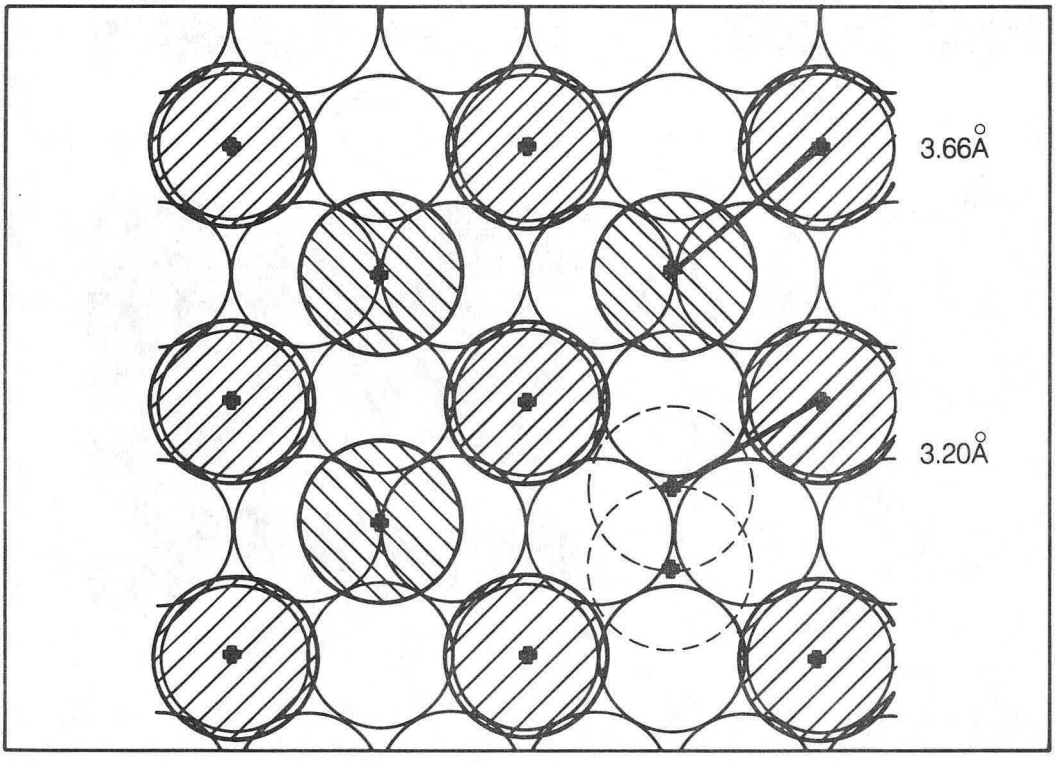

Top view

Pt (111)– c (4×2) – 2 CO
LEED Structure
at T = 150 K

XBL 857-3135

Fig. 2

Pt (III) – c (4×2) – 2 CO

R-factor contour plots

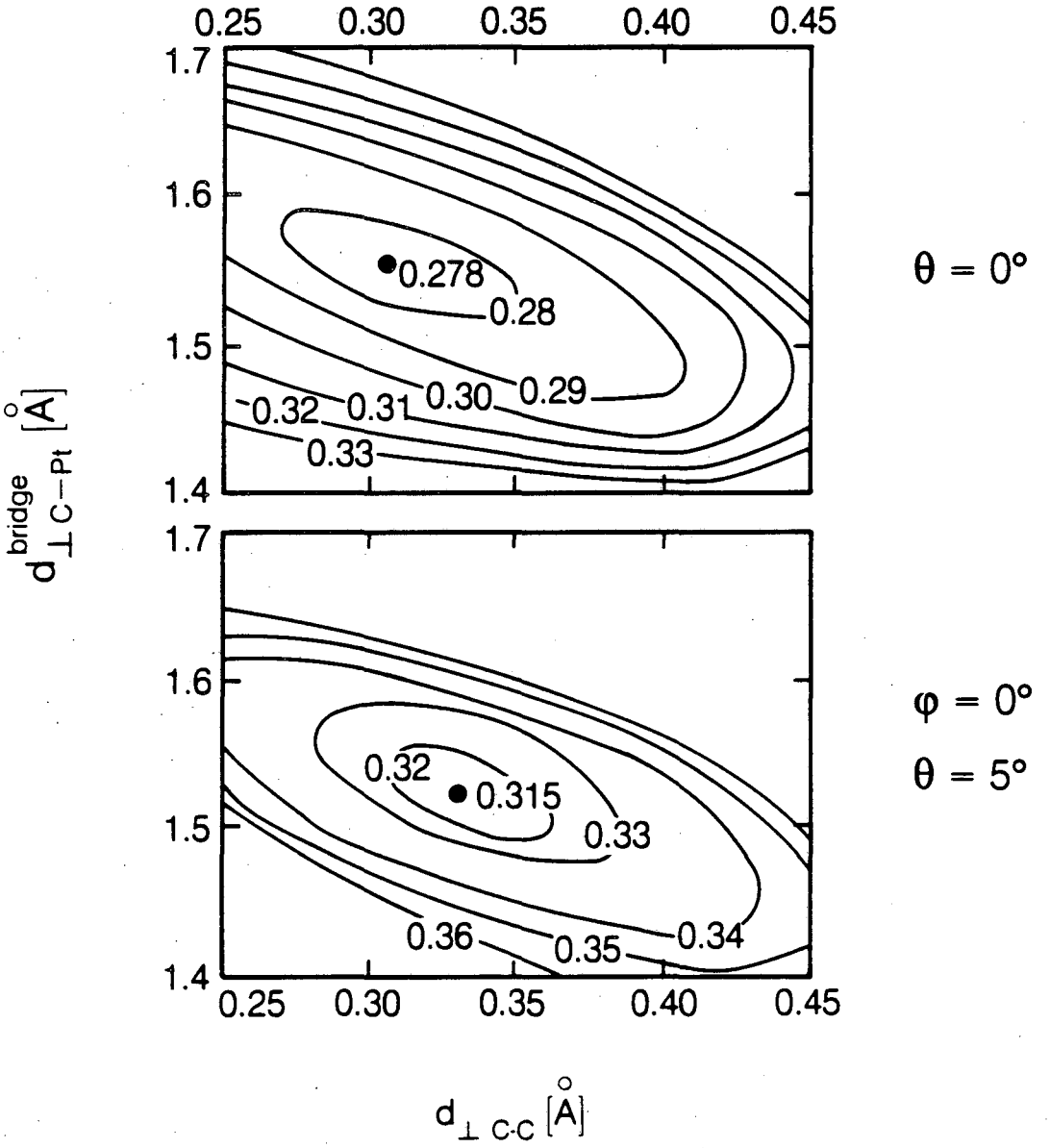

XBL 855–10512

Fig. 3

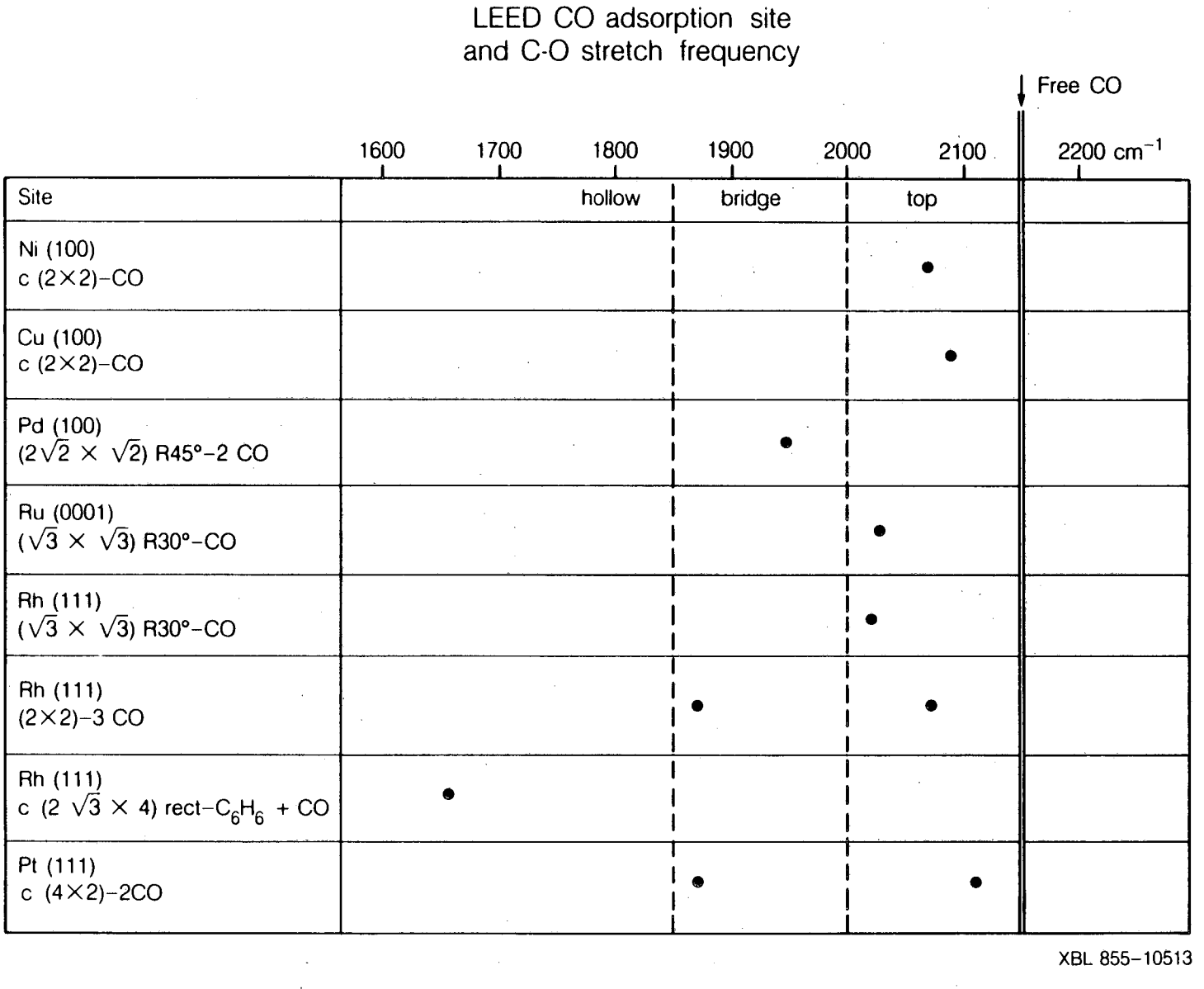
LEED CO adsorption site
and C-O stretch frequency
Free CO
1600
1700
1800
1900
2000
2100
2200 cm^{-1}
Site
hollow
bridge
top
Ni (100)
c (2×2)-CO
Cu (100)
c (2×2)-CO
Pd (100)
(2√2 × √2) R45°-2 CO
Ru (0001)
(√3 × √3) R30°-CO
Rh (111)
(√3 × √3) R30°-CO
Rh (111)
(2×2)-3 CO
Rh (111)
c (2 √3 × 4) rect-C_6H_6 + CO
Pt (111)
c (4×2)-2CO
XBL 855-10513

Fig. 4

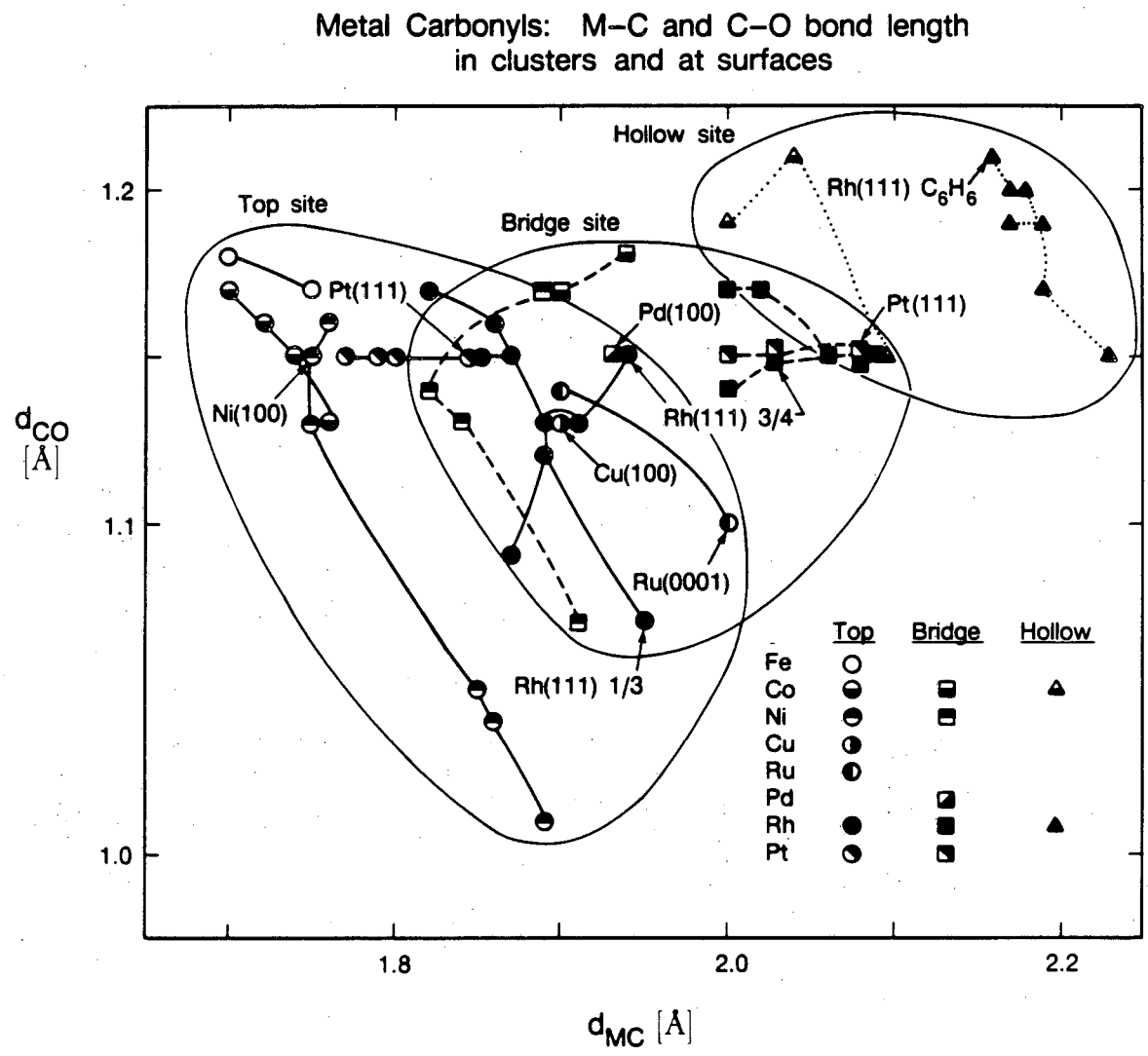
Metal Carbonyls: M–C and C–O bond length
in clusters and at surfaces
Hollow site
Top site
Bridge site
Rh(111) C_6H_6
Pt(111)
Pt(111)
Pd(100)
Ni(100)
Rh(111) 3/4
Cu(100)
Ru(0001)
Rh(111) 1/3
Top
Bridge
Hollow
Fe
Co
Ni
Cu
Ru
Pd
Rh
Pt
1.2
1.1
1.0
1.8
2.0
2.2
d_{CO} [Å]
d_{MC} [Å]
XBL 828-6271

Fig. 5

Metal carbonyls: Effective C radius in M-C bond and C-O bond length in clusters and at surfaces

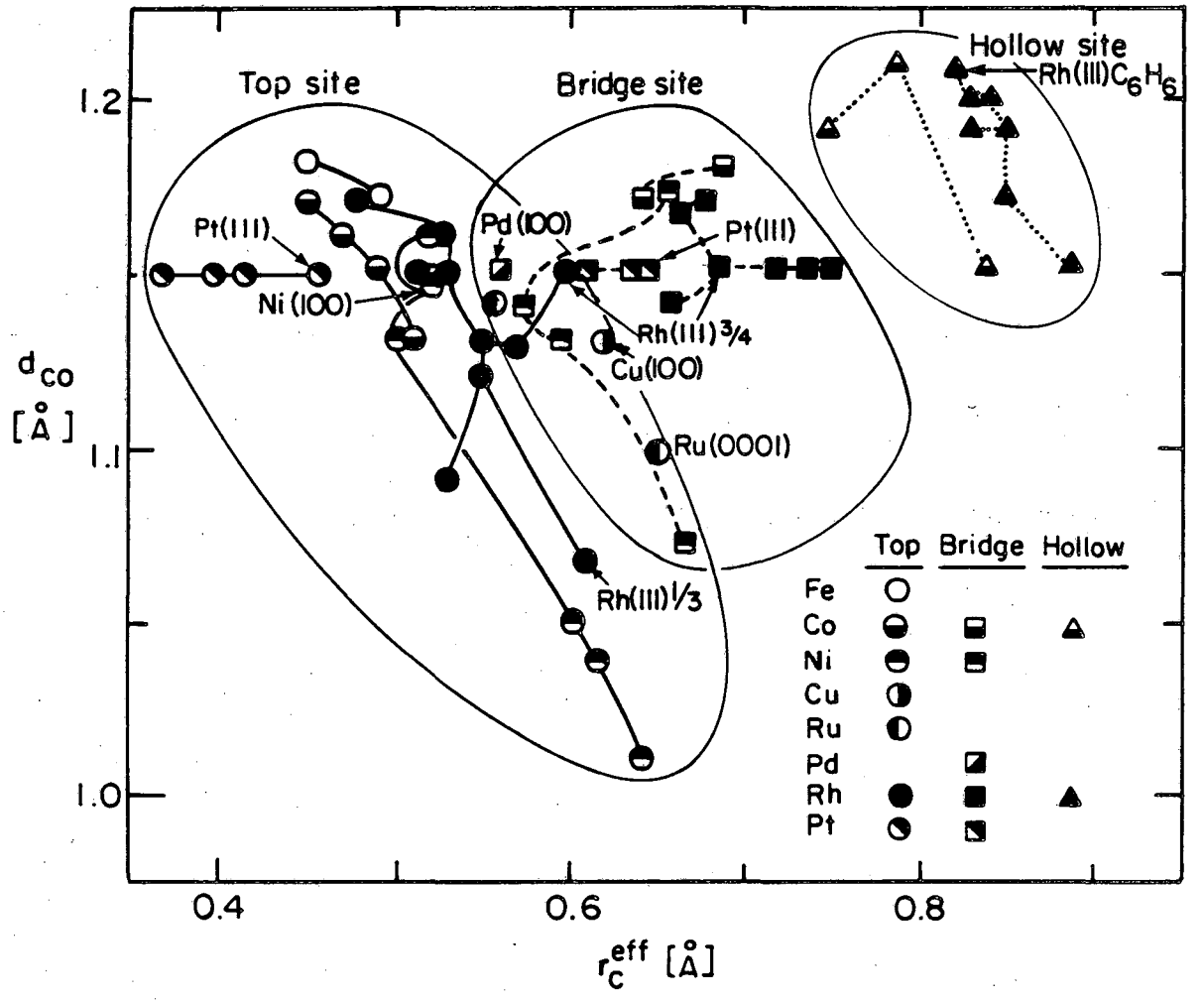

XBL828-6271

Fig. 6

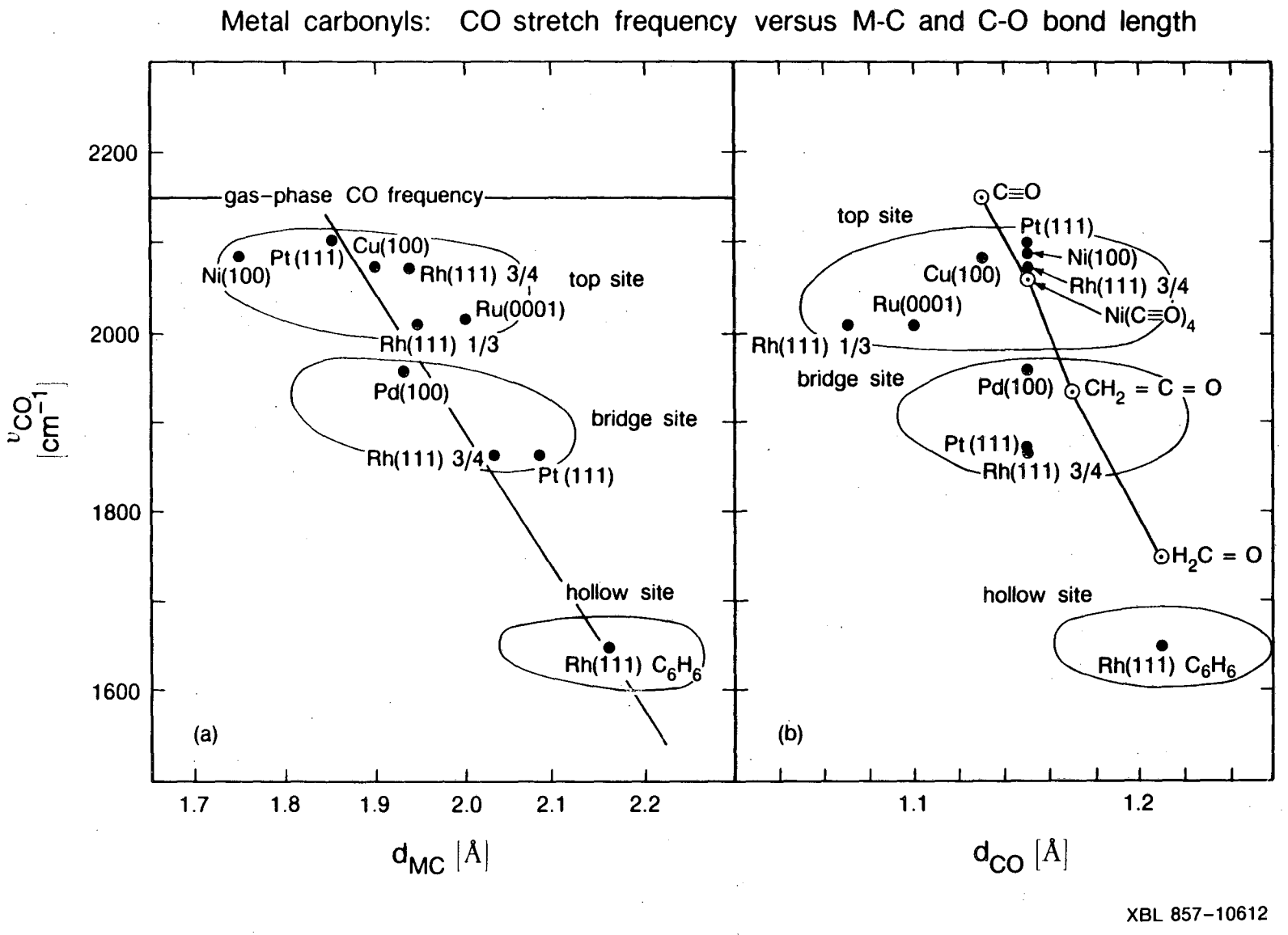
Metal carbonyls: CO stretch frequency versus M-C and C-O bond length
2200
2000
1800
1600
υ_{CO} [cm^{-1}]
gas-phase CO frequency
Ni(100)
Pt(111)
Cu(100)
Rh(111) 3/4
top site
Ru(0001)
Rh(111) 1/3
Pd(100)
bridge site
Rh(111) 3/4
Pt(111)
hollow site
Rh(111) C$_6$H$_6$
(a)
1.7
1.8
1.9
2.0
2.1
2.2
d_{MC} [Å]
C≡O
top site
Pt(111)
Ni(100)
Cu(100)
Rh(111) 3/4
Ru(0001)
Ni(C≡O)$_4$
Rh(111) 1/3
bridge site
Pd(100)
CH$_2$ = C = O
Pt(111)
Rh(111) 3/4
H$_2$C = O
hollow site
Rh(111) C$_6$H$_6$
(b)
1.1
1.2
d_{CO} [Å]
XBL 857-10612

Fig. 7

LAWRENCE BERKELEY LABORATORY
TECHNICAL INFORMATION DEPARTMENT
UNIVERSITY OF CALIFORNIA
BERKELEY, CALIFORNIA 94720